





Article

Multiple Fault Detection in Induction Motors through Homogeneity and Kurtosis Computation

Ana L. Martinez-Herrera, Edna R. Ferrucho-Alvarez, Luis M. Ledesma-Carrillo , Ruth I. Mata-Chavez , Misael Lopez-Ramirez  and Eduardo Cabal-Yepez * 

Multidisciplinary Studies Department, Engineering Division, Campus Irapuato-Salamanca, University of Guanajuato, Guanajuato 38944, Mexico; martinez.al@ugto.mx (A.L.M.-H.); er.ferruchoalvarez@ugto.mx (E.R.F.-A.); lm.ledesma@ugto.mx (L.M.L.-C.); ruth@ugto.mx (R.I.M.-C.); lopez.misael@ugto.mx (M.L.-R.)

* Correspondence: educabal@ugto.mx; Tel.: +52-445-458-9040

Abstract: In the last few years, induction motor fault detection has provoked great interest among researchers because it is a fundamental element of the electric-power industry, manufacturing enterprise, and services. Hence, considerable efforts have been carried out on developing reliable, low-cost procedures for fault diagnosis in induction motors (IM) since the early detection of any failure may prevent the machine from suffering a catastrophic damage. Therefore, many methodologies based on the IM startup transient current analysis have been proposed whose major disadvantages are the high mathematical complexity and demanding computational cost for their development. In this study, a straightforward procedure was introduced for identifying and classifying faults in IM. The proposed approach is based on the analysis of the startup transient current signal through the current signal homogeneity and the fourth central moment (kurtosis) analysis. These features are used for training a feed-forward, backpropagation artificial neural network used as a classifier. From experimentally obtained results, it was demonstrated that the brought-in scheme attained high certainty in recognizing and discriminating among five induction motor conditions, i.e., a motor in good physical condition (HLT), a motor with one broken rotor bar (1BRB), a motor with two broken rotor bars (2BRB), a motor with damage on the bearing outer race (BRN), and a motor with an unbalanced mechanical load (UNB).

Keywords: artificial neural network; fourth central moment; homogeneity analysis; induction motors; mechanical unbalance; one broken rotor bar; outer-race bearing fault; startup transient current; two broken rotor bars



Citation: Martinez-Herrera, A.L.; Ferrucho-Alvarez, E.R.; Ledesma-Carrillo, L.M.; Mata-Chavez, R.I.; Lopez-Ramirez, M.; Cabal-Yepez, E. Multiple Fault Detection in Induction Motors through Homogeneity and Kurtosis Computation. *Energies* **2022**, *15*, 1541. <https://doi.org/10.3390/en15041541>

Academic Editors: Mario Marchesoni and Ryszard Palka

Received: 4 January 2022

Accepted: 16 February 2022

Published: 19 February 2022

Publisher's Note: MDPI stays neutral with regard to jurisdictional claims in published maps and institutional affiliations.



Copyright: © 2022 by the authors. Licensee MDPI, Basel, Switzerland. This article is an open access article distributed under the terms and conditions of the Creative Commons Attribution (CC BY) license (<https://creativecommons.org/licenses/by/4.0/>).

1. Introduction

Induction motors have stayed for many years as essential components of every electrical and manufacturing process. Because of their low cost, stiffness, and quality of performing consistently well, they are extensively used around the planet. The squirrel cage induction motor (SCIM) provides the most common type of electromechanical drive for commercial, domestic, and, the most important, industrial applications, corresponding to around 85% of the electrical energy utilization in this area [1]. In the past decades, profound efforts have been devoted to induction motor (IM) fault diagnosis due to the economic and technical consequences of an unexpected downtime caused by a failure. As any other electrical device, an IM is vulnerable to numerous kinds of failures that can be classified as bearings' faults, with 50% of incidence, rotor faults, with the 10%, and stator-related faults, with the 40% [2]. Some of the symptoms produced by these failures are excessive vibrations, unbalanced line currents and/or voltages, torque pulsations and decreased average torque, and excessive heating, among others, aggravating efficiency losses on any process. Stator faults have been lessened at present by improving the SCIM design and its building quality. On the other hand, broken rotor bars (BRB), bearing faults

(BRN), and rotor unbalance (UNB) constitute very common problems, particularly in heavy duty systems [3]. Many efforts have been made to prevent catastrophic failures to occur with the application of several techniques for fault detection; unfortunately, most of them focus on detecting a single, specific fault separately, such as BRB [4], BRN [5], or UNB [6]. These techniques are usually based on monitoring and analyzing current and vibration signals [7]. Motor current signature analysis (MCSA) is one of the most popular and effective techniques for induction motor fault detection. It has the advantages of being noninvasive and simple to carry out, coming out with good results during faulty condition identification [8]. MCSA processes either the startup transient or the steady-state electric current signal fed to the SCIM stator, which is gathered with a current clamp probe to carry out early detection of these types of faults, trying to avoid unscheduled maintenance and interruption of production lines, which yield to critical outcomes in produced merchandise conditions, manufacturing prices, and security.

One of the most difficult faults to detect is broken rotor bars (BRB) because they usually do not lead to an abrupt total motor failure but to a progressive deterioration that may not be detected until the motor is severely damaged, causing a shutdown in the production line. In [9], a new technique was developed using the fast Fourier transform (FFT), and an index-based classifier was introduced for BRB diagnosis. Nevertheless, several studies have shown that analyzing the steady-state signal might not be an effective approach for identifying certain operational conditions such as voltage fluctuations, bearing failures, noise, and mechanical load changes [10]. Therefore, non-stationary signal analysis for SCIM fault detection has generated great interest in recent years. Some advantages of analyzing and monitoring the induction motor (IM) current signals during its transient state are related to the close relation between the signal noise and the rotor fast slip [7], making it easier to identify BRB and other kinds of faults during this regime. However, the greatest obstacle for this type of monitoring comes from the startup span, which is very short; besides that, non-stationary signals represent a challenging task as they cannot be analyzed separately in time or frequency domains. The short-time Fourier transform (STFT) [11] and the Hilbert transform [4] are well-known techniques for identifying faulty conditions in SCIM. On the other hand, the wavelet transform (WT) has attained great interest among researchers for BRB fault detection, as well as the high-resolution technique known as multiple signal classification (MUSIC) [12]. On the other hand, most of the techniques utilized for identifying bearing faults (BRN) rely on the analysis of vibration signals [5]. However, the STFT and the WT and its variations directly depend on the correct selection of a suitable window size and a mother wavelet function, respectively, to perform an effective signal analysis. Other works based on quadratic distributions (QD) [13–15] provide a time–frequency representation for non-stationary signals. However, QD may generate spurious frequencies called cross terms that compromise the correct identification of the fault-related frequencies. In an equivalent way, mechanical unbalance fault (UNB) diagnosis has been traditionally addressed by analyzing vibration signals [16–18], too.

Although the methods and techniques mentioned before are suitable for detecting and diagnosing independent induction motor faults, most of them rely on the combination of complex mathematical bases that demand specialized hardware and software for their implementation in order to take the time-domain signals into the frequency domain and back to the time domain. This requires a long execution time and computational resources for the signal processing. Furthermore, some of these techniques involve the analysis of the electric current from the three phases along with the multi-axis vibration signals from the SCIM. Therefore, in this study, an approach based on the examination of just one phase from the electrical current fed to the IM during its startup transient through homogeneity and kurtosis computations was presented for detecting and classifying distinct induction motor faults, i.e., one broken rotor bar (1BRB), two broken rotor bars (2BRB), a motor with damage on the bearing outer race (BRN), and a motor with an unbalanced mechanical load (UNB). The introduced methodology has a low computational complexity compared to other methods in related literature for signal examination aimed to IM fault detection;

hence, the proposed approach required a short processing time, making it feasible for being utilized in online-processing applications.

The paper is organized as follows. Section 2 provides a theoretical background for fault and indexes' description. Section 3 describes the experimental setup. Section 4 presents the obtained results, and, finally, some conclusions are provided in Section 5.

2. Theoretical Framework

This section provides a mathematical background about the induction motor faults treated in this work, as well as the signal processing techniques utilized for analyzing the startup electric current signal and the artificial neural network utilized for classifying the IM operational condition.

2.1. Broken Rotor Bar Fault (BRB)

The BRB fault is the most common rotor-related failure that affects SCIM, and it is very difficult to detect because, under this state, the motor operates apparently under normal condition. BRB is mainly caused by overload and thermal imbalances, electromagnetic forces and noise, vibrations, environmental damage, or by manufacturing processes.

An induction motor operating with BRB defects generates an opposing succession of rotor currents caused by the asymmetries, which bring on a distinctive element in the frequency spectrum of the stator current. The fault-related frequencies (f_{BRBs}) indicating the presence of BRB are given by:

$$f_{BRBs} = (1 - 2ks)f_s, \quad k = 1, 2, 3, \dots \quad (1)$$

where k is an integer number, f_s is the main frequency component of the electric power supply, and the motor slip is represented by s , which takes values in the range from 0 to 1 [19].

2.2. Bearing Fault (BRN)

Characteristic frequency components are generated on the stator current when an SCIM has a faulty bearing. These specific frequency components can be predicted since they are related to both the power supply frequency and the mechanical system frequency. When there is a fault in any component of a bearing, for instance, its inner raceway, outer raceway, or rolling elements, specific components are induced in the vibration and current signals of the machine. These characteristic frequencies associated to the bearing faults depend directly on the bearing geometry and the machine rotating speed. A defect on the outer race will cause an impulse every time the rolling elements make contact with the defect. The outer raceway-related frequency can be theoretically determined by

$$f_o = \frac{n}{2}f_r \left[1 - \left(\frac{BD}{PD} \right) \cos(\beta) \right] \quad (2)$$

where n is the number of balls (rolling elements), f_r is the shaft rotating frequency, BD is the diameter of the balls, PD is the bearing race diameter, and β is the angle between the ball in the race [20].

2.3. Mechanical Unbalance Fault (UNB)

When the mechanical load of the induction motor is not evenly disseminated, displacing the center of mass out of the motor rotating axis, there is an unbalance fault. A manufacturing defect is the principal cause of rotor unbalance; also, heating dilation has an effect on the internal misalignment or the shaft deviation that produces an unbalanced rotor. The unbalance state occurs when there is an uneven distribution of weight around the rotor center of rotation, generating an unbalance force U , which is given by

$$U = m \times r \quad (3)$$

where m is the mass and r is its eccentricity, which is the separation between the rotor center of mass and its rotating axis. Unbalance force fluctuates with the rotating speed and drags the rotor off from the stator center bore to a distinct position, which is known as the heavy spot. Mutual inductances between stator and rotor loops get to be uneven because of the rotor unbalance, which results in frequency components induced in the stator current that are given by

$$f_{unb} = f_s[1 \pm k(1 - s)/p], \quad k = 1, 2, 3, \dots \quad (4)$$

where f_s is the fundamental frequency of the electric current supply, k is an integer number, s is the motor slip, and p is the number of pole pairs in the SCIM [21].

2.4. Homogeneity

In image classification, homogeneity is a textural attribute that estimates the variability of the gray level in the pixels from an image. It is derived from the gray level co-occurrence matrix (GLCM) [22], and it measures the closeness of the element distribution in the GLCM regarding its diagonal. The GLCM shows how many times each gray level comes about at a pixel situated at a predetermined geometric position regarding any other pixel through a function of their gray levels. Homogeneity ranges from 0 to 1 and reaches its maximum value when the diagonal elements have a value of 1. Homogeneity can be computed by

$$H = \sum_i \sum_j \frac{1}{1 + (i - j)^2} p(i, j) \quad (5)$$

where $p(i, j)$ is the (i, j) th element of the normalized GLCM. Homogeneity can be used as an index for fault detection and classification in SCIM since distinct fault-associated frequency elements are induced in the electrical current signal, changing its uniformity [23].

2.5. Kurtosis

Kurtosis has the capability of measuring the deviation, i.e., tailedness, of a probability distribution, and discriminating between distributions with different shapes; therefore, it can be used as an efficient indicator for SCIM fault detection. Kurtosis is the fourth-order moment that describes the shape of a probability distribution from a signal. If there is a high impulsive component, with a sharp signal intensity distribution, then there is a high kurtosis value. Kurtosis of a random event X is computed as

$$Kurt[X] = \frac{\frac{1}{N} \sum_{i=1}^N (x_i - \mu)^4}{\left(\frac{1}{N} \sum_{i=1}^N (x_i - \mu)^2\right)^2} = \frac{\mu_4}{\sigma^4} \quad (6)$$

where N is the number of samples, x_i is the time raw-signal sample for $i = 1, 2, \dots, N$, and μ is the mean of the random event $X = [x_1, x_2, x_3, \dots, x_N]$.

2.6. Artificial Neural Networks

Artificial neural networks (ANN) provide a powerful and speedy tool for classification problems. Figure 1 shows the basic design of ANN with two layers where each neuron produces a unique number. Inputs are multiplied by corresponding weights and summed up. The corresponding output is derived after adding a bias term to the in-between results. The sum of the weighted inputs is transformed through a nonlinear activation function to get the outcome of each corresponding neuron. Several triggering functions are viable; however, in this work, from an empirical analysis, a hyperbolic tangent function was used. The multilayer perceptron architecture is used in the ANN during experimentation. It is made up of a feed-forward architecture composed of an input layer, one or more inside layers, and one output layer. The number of inside layers and neurons on each layer is determined by the dealt issue; in this case, the inputs correspond to the signal-obtained features, i.e., homogeneity and kurtosis. The hidden layer is set heuristically

by experimentation, whereas the number of output neurons is related to the distinct categories being recognized. The ANN employed in this experimentation was trained using a Levenberg–Marquardt backpropagation scheme [24].

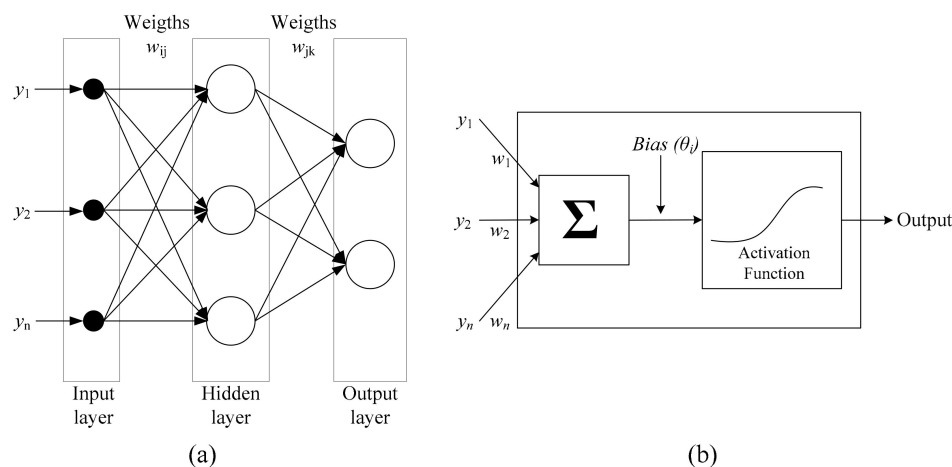


Figure 1. (a) Typical scheme of an ANN, (b) operation of an artificial neuron in a layer.

3. Experimentation

The electrical current signal from the startup transient of a SCIM is used for identifying and classifying a healthy motor (HLT) or a motor with a faulty condition from those treated in this study, i.e., one broken rotor bar (1BRB), two broken rotor bars (2BRB), outer-race faulty bearing (BRN), and mechanical unbalance (UNB). Figure 2 shows the testbench configuration, which employs distinct 1-HP SCIM (model WEG 00136APE48T) for assessing the feasibility of using the introduced procedure to identify and classify distinct operational states.

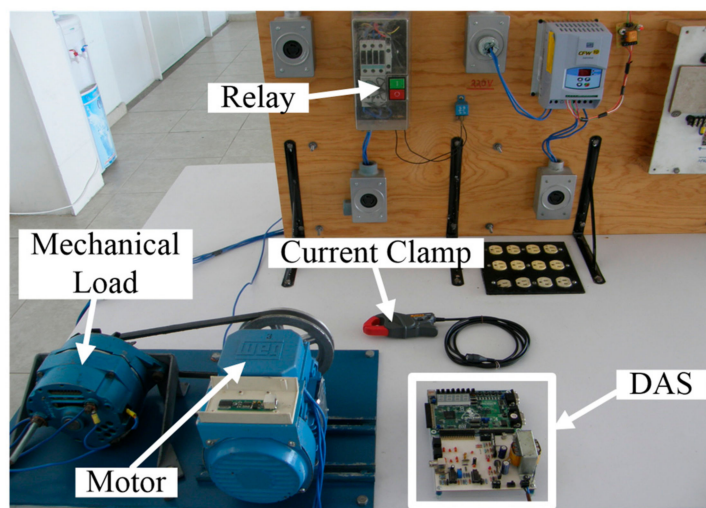


Figure 2. Testbench used for assessing the proposed method for detecting and classifying distinct faults in SCIM.

The motors under test received an electric power supply of 220 V ac at 60 Hz. They had 28 bars in the rotor, two poles, and the used mechanical load was an ordinary alternator that was equivalent to one-quarter of the SCIM nominal load. One phase of the three-phase electric current supply signal was collected through an i200s, ac current clamp from Fluke. The data acquisition system (DAS) used a 16-bit analog-to-digital converter (ADS7809). The instrumentation system used a sampling frequency f_0 of 1.5 kHz, obtaining 4096 samples in 2.7 s during the induction motor startup transient.

For this study, one motor was kept in healthy condition, i.e., in good physical condition, to be used as benchmark. The 1BRB and 2BRB conditions were generated in a synthetic way by drilling one hole and two holes, respectively, with a diameter of 7.938 mm, without damaging the rotor shaft, as shown in Figure 3a,b, respectively. On the other hand, the bearing was synthetically harmed on its outer race by boring a 1.191-mm hole utilizing a tungsten drill bit. Figure 3c displays the bearing model 6203-2ZNR that was synthetically damaged to carry out the experimentation. The mechanical unbalance fault was generated by adding a mass in one of the pulley arms. In a drilled hole with 8 mm of diameter, a two-sided screw was placed and secured using female screws on both sides of the pulley arm, as depicted in Figure 3d. A total of 100 trials were executed for each motor condition.

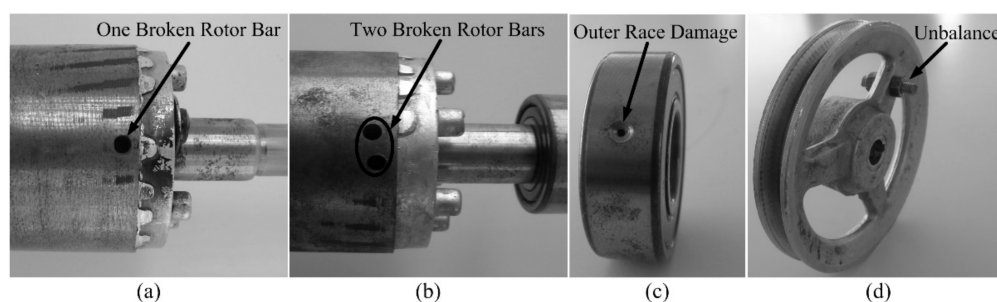


Figure 3. Artificially generated faults. (a) One broken rotor bar (1BRB); (b) two broken rotor bars (2BRB); (c) bearing with outer race damaged (BRN), and (d) mechanical unbalance.

Figure 4 depicts the proposed methodology for multiple fault diagnosis and classification. The electrical current signal of the startup transient was obtained by the current clamp; then, it was adjusted and analog-to-digital transformed in the DAS. The resulting discrete current signal was treated for obtaining the desired features, homogeneity and kurtosis, which were used as entries to the artificial neural network, a multilayer perceptron with a feed-forward architecture.

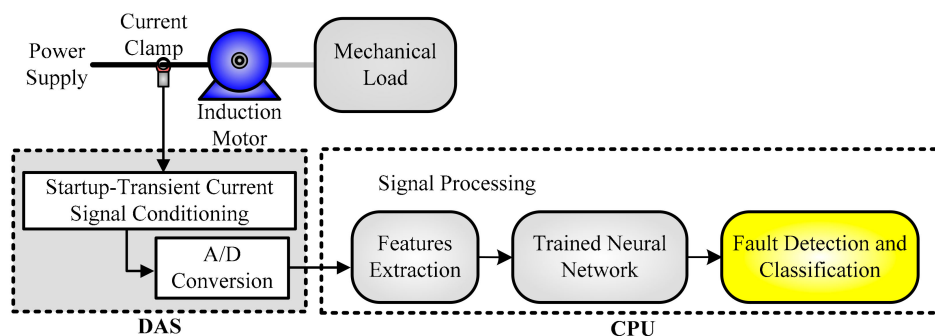


Figure 4. Proposed approach for distinct fault detection and classification.

Homogeneity and kurtosis values were obtained and normalized for each motor condition by the definitions (5) and (6), respectively. For each motor condition, a statistical analysis was performed. The mean (μ) and standard deviation (σ) of the homogeneity and kurtosis values for a motor without harm (HLT), a motor with one separated rotor bar (1BRB), a motor with two shattered rotor bars (2BRB), a motor with outer-race bearing damage (BRN), and a motor with unbalance (UNB) show that the respective probability density functions (PDF) partially cover each other in some degree, impeding a direct classification. Figure 5 shows the PDF of homogeneity and kurtosis features where the overlap among some of the treated conditions is evident. Therefore, a neural network classification was used for refining the proper operation that allowed a precise identification of multiple operational conditions.

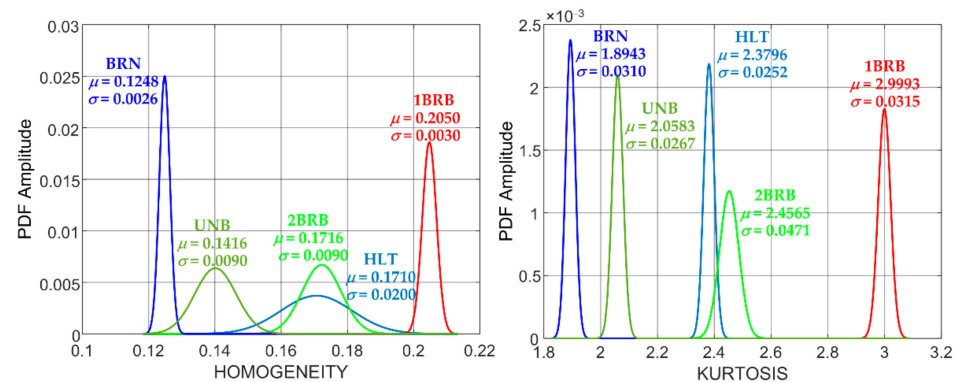


Figure 5. Homogeneity and kurtosis PDF values for the different motor states: HLT, healthy; 1BRB, one broken rotor bar; 2BRB, two broken rotor bars; BRN, outer-race bearing damage; and UNB, unbalance.

The classification was carried out utilizing the homogeneity and kurtosis data as entries to the ANN. The artificial neural network was a multilayer perceptron with a feed-forward architecture with two inputs (kurtosis values and homogeneity values) only, one hidden layer, and one output. A Levenberg–Marquardt backpropagation algorithm was used for training the ANN and the mean-square-error index was used for performance assessment. Inputs to the ANN were the feature vectors composed of the homogeneity and kurtosis data, where each motor condition had a total of 20 values in its validation data set, given as a result of feature vectors of length 100.

4. Obtained Results

The proposed technique efficacy was validated through 100 different trials under each treated motor condition. A holdout-type data set was employed, where the first 70 experiments were employed for teaching the network and the remaining ones were used for checking the proposed methodology efficacy. Table 1 shows the performance results, through a confusion matrix, of the introduced technique during the identification and classification of the IM operational condition as HLT, 1BRB, 2BRB, BRN, and UNB. The right-most column in Table 1 displays the average success rate of the suggested procedure.

The results obtained experimentally are depicted in Table 1 and they show that the introduced methodology reached 100% of effectiveness on identifying and discriminating among a healthy motor (HLT), a motor with one broken rotor bar (1BRB), a motor with two broken rotor bars (2BRB), a motor with outer-race bearing damage (BRN), and a motor with an unbalanced mechanical load (UNB). The proposed technique was executed in a 2.20-GHz Intel Core i7-8750 processor, making use of the software MATLAB 2020a.

Table 1. Confusion matrix and overall effectiveness of using homogeneity and kurtosis features for fault detection and classification in SCIM.

IM Condition	HLT	1BRB	2BRB	BRN	UNB	Overall Effectiveness
HLT	20	0	0	0	0	100%
1BRB	0	20	0	0	0	100%
2BRB	0	0	20	0	0	100%
BRN	0	0	0	20	0	100%
UNB	0	0	0	0	20	100%

Discussion

The proposed methodology is compared against previous approaches used for detecting SCIM faults in Table 2. The obtained results from real experimentation demonstrated the usefulness of homogeneity and kurtosis as indexes for IM diagnosis and their high reliability as indicators for multiple fault identification and classification [25,26]. The proposed

approach can recognize and classify the operational condition of an induction motor as in a good state (HLT), a motor with one split rotor bar (1BRB), a motor with two damaged rotor bars (2BRB), a motor with outer race damage in the bearing (BRN), and a motor with an unbalanced mechanical load (UNB) with high certainty, attaining up to 100% of effectiveness, utilizing just two features of a single phase from the three-phase electrical current supply to the SCIM, as inputs to a multilayer perceptron ANN. This is different from other approaches reported in the reviewed literature that even require the signal transformation from the time domain into the frequency domain and back to the time domain to carry out the signal processing in order to extract up to 29 features of the current signals from the three phases and the multi-axis vibration signals, in conjunction, in order to be capable of performing the fault detection. In the proposed procedure, the electrical current signal from the SCIM startup transient was analyzed just in time domain without any pre-treatment, which is an evident convenience compared to the previous works in Table 2, which require the combination of two or more processing techniques to carry out a qualitative diagnosis or to perform it in a quantitative style by analyzing current and vibration signals in time, frequency, and even time-frequency domains. Therefore, the proposed methodology is a reliable tool that ensures high certainty during different fault detections and classifications in induction motors through the analysis of just one phase from startup electric current supply, outperforming previous approaches in the state of the art.

Table 2. Comparison chart of the proposed methodology against the state of the art in related literature for fault detection in IM.

Method	Accuracy Rate	Applied Techniques	Detected Fault
Garcia-Bracamonte et al. [8]	From 90% to 99%	Autocorrelation; FFT; independent component analysis; region-of-interest segmentation; and 1-D, 2-D, and 3-D vector extraction.	
Yang and Shi [27]	Qualitative	Wavelet packet, threshold optimization, Shannon entropy, wavelet packet reconstruction, and FFT computation.	
Haroun et al. [28]	From 81.4% to 100%	Zero-crossing time, envelope extraction of the three phase currents, frequency domain characterization, ReliefF algorithm, and self-organizing map.	BRB only
Li et al. [29]	Qualitative	Fourier transform, power spectral density estimation, local characteristic frequency bands' synchronization, spectrum transformation, central point computation, and kurtosis energy-based spectrum.	
Gong et al. [30]	Qualitative	Wavelet packet transform and spectral kurtosis.	
Gao and Xiang [31]	Qualitative	Ensemble empirical mode decomposition, L-Kurtosis value, FFT, clustering-based segmentation, inverse FFT, and Hilbert envelope spectrum computation.	BRN only
Navasari et al. [32]	From 98% to 100%	Wavelet decomposition, sampling of the decomposition streams, energy computation, and ANN.	
Ben Abid et al. [33]	100%	Stationary wavelet packet transform, root mean square (RMS), aiNet clustering algorithm, and directed acyclic graph support vector machine.	
Rahman and Uddin [16]	Qualitative	Standard deviation, crest factor, and kurtosis computation; FFT; DWT-based frequency domain analysis; Hilbert transform; and envelope detection.	
Tahir et al. [17]	100%	Multi-axis RMS value, variance, skewness, kurtosis, impulse factor, and range computation; signed distance computation; and SVM.	UNB only
Guo et al. [18]	86.87%	DC part removal, signal resampling, continuous wavelet transform scalogram (CWTS), cropping, and convolutional neural network.	
Cunha Palacios et al. [34]	From 99.7% to 100%	Signal segmentation, peak value, module computation, crossover detection, normalization, input selection, classification through different intelligent algorithms.	BRN, BRB, and Stator Faults
Jigyasu et al. [35]	From 99.7% to 100%	RMS, variance, kurtosis, peak value, skewness, median, crest factor, margin factor, impulse factor, shape, and median range extraction; different neural network structures.	BRN, BRB, and Eccentricity
Proposed Approach	100%	Homogeneity, kurtosis, and an ANN.	1BRB, 2BRB, BRN, and UNB

5. Conclusions

Recently proposed techniques can detect one single induction motor fault with an adequate certainty; however, most of them rely on the combination of complex mathematical operations that require specific hardware and software for their implementation. Furthermore, they involve the monitoring and processing of different signals as electric current supply and multi-axis vibration signals to obtain time, frequency, and even time–frequency features that allow them to attain high certainty on the induction motor diagnosis. Therefore, in this work, a straightforward technique for multiple IM fault detection, which just requires the computation of homogeneity and kurtosis from a single phase of the supplied electrical current signal during the SCIM startup transient, was introduced. The obtained results from experimental studies demonstrated that the proposed methodology provides highly reliable results on detecting and classifying distinct induction motor faults by computing the homogeneity and kurtosis on the time domain, allowing the identification of five different operational conditions, a motor in healthy state (HLT), a motor with one broken bar (1BRB), a motor with two broken rotor bars (2BRB), a motor with outer-race damage on its bearing (BRN), and a motor with an unbalanced mechanical load (UNB), with remarkable certainty. A thorough comparison against the state of the art in the subject of induction motor fault detection showed that the proposed method outperformed previous approaches in the reviewed literature, which usually just detect one single type of fault, by implementing a low-cost computational technique suitable for online applications.

Future work will focus on assessing the proposed technique for multiple IM fault detection under different scenarios. It will contemplate incorporating additional faulty conditions and signal examination techniques to recover other signal characteristics, as well as assessing distinct kinds of classifications to carry out the fault identification and sorting with high precision.

Author Contributions: A.L.M.-H. and E.R.F.-A. performed the methodology implementation and helped during experimentation for data acquisition. L.M.L.-C. helped during data analysis and result interpretation. R.I.M.-C. helped during the manuscript writing—review and editing. M.L.-R. helped during experimentation and data acquisition. E.C.-Y. supervised the project and the experimentation implementation, assessed the obtained results, and helped in the document preparation. All authors have read and agreed to the published version of the manuscript.

Funding: This research received no external funding.

Institutional Review Board Statement: Not applicable.

Informed Consent Statement: Not applicable.

Acknowledgments: This work was supported in part by the National Council on Science and Technology (CONACYT), Mexico, under Grants 443689 and 710888, and in part by DAIP—U. de Gto. under the Convocatoria Institucional de Investigacion Cientifica 2022.

Conflicts of Interest: The authors declare no conflict of interest.

References

1. Hassan, O.E.; Amer, M.; Abdelsalam, A.K.; Williams, B.W. Induction Motor Broken Rotor Bar Fault Detection Techniques Based on Fault Signature Analysis—A Review. *IET Electr. Power Appl.* **2018**, *12*, 895–907. [[CrossRef](#)]
2. Thomson, W.T.; Fenger, M. Current Signature Analysis to Detect Induction Motor Faults. *IEEE Ind. Appl. Mag.* **2001**, *7*, 26–34. [[CrossRef](#)]
3. Cubert, J.M. Use of Electronic Controllers in Order to Increase the Service Life on Asynchronous Motors. In Proceedings of the European Seminar on Electro-Technologies for Industry, Bilbao, Spain, 20–22 May 1992; pp. 393–404.
4. Abd-el-Malek, M.B.; Abdelsalam, A.K.; Hassan, O.E. Novel Approach Using Hilbert Transform for Multiple Broken Rotor Bars Fault Location Detection for Three Phase Induction Motor. *ISA Trans.* **2018**, *80*, 439–457. [[CrossRef](#)] [[PubMed](#)]
5. Deekshit Kompella, K.C.; Venu Gopala Rao, M.; Srinivasa Rao, R. Bearing Fault Detection in a 3 Phase Induction Motor Using Stator Current Frequency Spectral Subtraction with Various Wavelet Decomposition Techniques. *Ain Shams Eng. J.* **2018**, *9*, 2427–2439. [[CrossRef](#)]

6. Rahman, M.M.; Uddin, M.N. Online Unbalanced Rotor Fault Detection of an IM Drive Based on Both Time and Frequency Domain Analyses. In Proceedings of the 2015 Industry Applications Society Annual Meeting, Addison, TX, USA, 18–22 October 2015; pp. 1–8. [[CrossRef](#)]
7. Liu, Y.; Bazzi, A. A Review and Comparison of Fault Detection and Diagnosis Methods for Squirrel-Cage Induction Motors: State of the Art. *ISA Trans.* **2017**, *70*, 400–409. [[CrossRef](#)] [[PubMed](#)]
8. Garcia-Bracamonte, J.E.; Ramirez-Cortes, J.M.; de Rangel-Magdaleno, J.J.; Gomez-Gil, P.; Peregrina-Barreto, H.; Alarcon-Aquino, V. An Approach on MCSA-Based Fault Detection Using Independent Component Analysis and Neural Networks. *IEEE Trans. Instrum. Meas.* **2019**, *68*, 1353–1361. [[CrossRef](#)]
9. Rivera-Guillen, J.R.; De Santiago-Perez, J.J.; Amezquita-Sanchez, J.P.; Valtierra-Rodriguez, M.; Romero-Troncoso, R.J. Enhanced FFT-Based Method for Incipient Broken Rotor Bar Detection in Induction Motors during the Startup Transient. *Measurement* **2018**, *124*, 277–285. [[CrossRef](#)]
10. Zajac, M.; Sulowicz, M. Wavelet Detectors for Extraction of Characteristic Features of Induction Motor Rotor Faults. In Proceedings of the 2016 International Conference on Signals and Electronic Systems (ICSES), Krakow, Poland, 5–7 September 2016; pp. 212–218. [[CrossRef](#)]
11. Ayon-Sicaeros, R.A.; Cabal-Yepez, E.; Ledesma-Carrillo, L.M.; Hernandez-Gomez, G. Broken-Rotor-Bar Detection Through STFT and Windowing Functions. In Proceedings of the 2019 IEEE Sensors Applications Symposium (SAS), Sophia Antipolis, France, 11–13 March 2019; pp. 1–5. [[CrossRef](#)]
12. Bensaoucha, S.; Bessedik, S.A.; Ameer, A.; Moreau, S.; Teta, A. A Comparative Study for Broken Rotor Bars Fault Detection in Induction Machine Using DWT and MUSIC Techniques. In Proceedings of the 2020 1st International Conference on Communications, Control Systems and Signal Processing (CCSSP), El Oued, Algeria, 16–17 May 2020; pp. 523–528. [[CrossRef](#)]
13. Climente-Alarcon, V.; Antonino-Daviu, J.A.; Riera-Guasp, M.; Vlcek, M. Induction Motor Diagnosis by Advanced Notch FIR Filters and the Wigner–Ville Distribution. *IEEE Trans. Ind. Electron.* **2014**, *61*, 4217–4227. [[CrossRef](#)]
14. Perez-Ramirez, C.A.; Amezquita-Sanchez, J.P.; Dominguez-Gonzalez, A.; Valtierra-Rodriguez, M.; Camarena-Martinez, D. Compact Kernel Distribution-Based Approach for Broken Bars Detection on Induction Motors. In Proceedings of the 2015 IEEE International Autumn Meeting on Power, Electronics and Computing (ROPEC), Ixtapa, Mexico, 4–6 November 2015; pp. 1–6. [[CrossRef](#)]
15. Quinde, I.R.; Sumba, J.C.; Ochoa, L.E.; Guevara, A.V., Jr.; Morales-Menendez, R. Bearing Fault Diagnosis Based on Optimal Time-Frequency Representation Method. *IFAC-PapersOnLine* **2019**, *52*, 194–199. [[CrossRef](#)]
16. Rahman, M.M.; Uddin, M.N. Online Unbalanced Rotor Fault Detection of an IM Drive Based on Both Time and Frequency Domain Analyses. *IEEE Trans. Ind. Appl.* **2017**, *53*, 4087–4096. [[CrossRef](#)]
17. Tahir, M.M.; Hussain, A.; Badshah, S.; Khan, A.Q.; Iqbal, N. Classification of Unbalance and Misalignment Faults in Rotor Using Multi-Axis Time Domain Features. In Proceedings of the 2016 International Conference on Emerging Technologies (ICET), Islamabad, Pakistan, 18–19 October 2016; pp. 1–4. [[CrossRef](#)]
18. Guo, S.; Yang, T.; Gao, W.; Zhang, C. A Novel Fault Diagnosis Method for Rotating Machinery Based on a Convolutional Neural Network. *Sensors* **2018**, *18*, 1429. [[CrossRef](#)] [[PubMed](#)]
19. Burnett, R.; Watson, J.F.; Elder, S. The Application of Modern Signal Processing Techniques for Use in Rotor Fault Detection and Location within Three-Phase Induction Motors. *Signal Process.* **1996**, *49*, 57–70. [[CrossRef](#)]
20. Frosini, L.; Bassi, E. Stator Current and Motor Efficiency as Indicators for Different Types of Bearing Faults in Induction Motors. *IEEE Trans. Ind. Electron.* **2010**, *57*, 244–251. [[CrossRef](#)]
21. Benbouzid, M.E.H.; Vieira, M.; Theys, C. Induction Motors’ Faults Detection and Localization Using Stator Current Advanced Signal Processing Techniques. *IEEE Trans. Power Electron.* **1999**, *14*, 14–22. [[CrossRef](#)]
22. Haralick, R.M.; Shanmugam, K.; Dinstein, I. Textural Features for Image Classification. *IEEE Trans. Syst. Man Cybern.* **1973**, *SMC-3*, 610–621. [[CrossRef](#)]
23. Sapena-Bano, A.; Pineda-Sanchez, M.; Puche-Panadero, R.; Martinez-Roman, J.; Matic, D. Fault Diagnosis of Rotating Electrical Machines in Transient Regime Using a Single Stator Current’s FFT. *IEEE Trans. Instrum. Meas.* **2015**, *64*, 3137–3146. [[CrossRef](#)]
24. Kowalski, C.T.; Orłowska-Kowalska, T. Neural Networks Application for Induction Motor Faults Diagnosis. *Math. Comput. Simul.* **2003**, *63*, 435–448. [[CrossRef](#)]
25. Yang, R.; Li, H.-K.; Tang, D.-L.; Hou, M.-F. Based on the Optimal Frequency Band of Maximum Correlation Kurtosis Deconvolution for Bearing Weak Fault Diagnosis. In Proceedings of the 2017 Prognostics and System Health Management Conference (PHM-Harbin), Harbin, China, 9–12 July 2017; pp. 1–5. [[CrossRef](#)]
26. Lizarraga-Morales, R.A.; Rodriguez-Donate, C.; Cabal-Yepez, E.; Lopez-Ramirez, M.; Ledesma-Carrillo, L.M.; Ferrucho-Alvarez, E.R. Novel FPGA-Based Methodology for Early Broken Rotor Bar Detection and Classification Through Homogeneity Estimation. *IEEE Trans. Instrum. Meas.* **2017**, *66*, 1760–1769. [[CrossRef](#)]
27. Yang, M.; Shi, W. Research on Feature Extraction Method for Motor Rotor Broken Bar Based on Optimized Wavelet Packet Analysis. In Proceedings of the 2018 IEEE 4th Information Technology and Mechatronics Engineering Conference (ITOEC), Chongqing, China, 14–16 December 2018; pp. 24–28. [[CrossRef](#)]
28. Haroun, S.; Nait Seghir, A.; Touati, S. Self-Organizing Map and Feature Selection for IM Broken Rotor Bars Faults Detection and Diagnosis. In Proceedings of the 2018 International Conference on Electrical Sciences and Technologies in Maghreb (CISTEM), Algiers, Algeria, 28–31 October 2018; pp. 1–6. [[CrossRef](#)]

29. Li, D.D.; Wang, W.; Ismail, F. An Energy Spectral Technique for Induction Motor Fault Detection. In Proceedings of the 2017 International Conference on Sensing, Diagnostics, Prognostics, and Control (SDPC), Shanghai, China, 16–18 August 2017; pp. 704–709. [[CrossRef](#)]
30. Gong, X.; Zhang, W.; Jing, Y.; Du, W.; Jing, Y. Bearing Fault Diagnosis for Coupling Faults of Rotor System Using Spectral Kurtosis and Wavelet Packet. In Proceedings of the 2019 International Conference on Sensing, Diagnostics, Prognostics, and Control (SDPC), Beijing, China, 15–17 August 2019; pp. 479–483. [[CrossRef](#)]
31. Gao, Q.; Xiang, J. A Method Using EEMD and L-Kurtosis to Detect Faults in Roller Bearings. In Proceedings of the 2018 Prognostics and System Health Management Conference (PHM-Chongqing), Chongqing, China, 26–28 October 2018; pp. 71–76. [[CrossRef](#)]
32. Navasari, E.; Asfani, D.A.; Negara, M.Y. Detection of Induction Motor Bearing Damage with Starting Current Analysis Using Wavelet Discrete Transform and Artificial Neural Network. In Proceedings of the 2018 10th International Conference on Information Technology and Electrical Engineering (ICITEE), Bali, Indonesia, 24–26 July 2018; pp. 316–319. [[CrossRef](#)]
33. Ben Abid, F.; Zgarni, S.; Braham, A. Distinct Bearing Faults Detection in Induction Motor by a Hybrid Optimized SWPT and AiNet-DAG SVM. *IEEE Trans. Energy Convers.* **2018**, *33*, 1692–1699. [[CrossRef](#)]
34. Cunha Palácios, R.H.; da Silva, I.N.; Goedel, A.; Godoy, W.F. A Comprehensive Evaluation of Intelligent Classifiers for Fault Identification in Three-Phase Induction Motors. *Electr. Power Syst. Res.* **2015**, *127*, 249–258. [[CrossRef](#)]
35. Jigyasu, R.; Mathew, L.; Sharma, A. Multiple Faults Diagnosis of Induction Motor Using Artificial Neural Network. In Proceedings of the 2018 Second International Conference (ICAICR), Shimla, India, 14–15 July 2018; pp. 701–710. [[CrossRef](#)]